scientific reports

Check for updates

OPEN

Green synthesis of silver nanoparticles by *Smyrnium cordifolium* plant and its application for colorimetric detection of ammonia

Mohammad Amin Rashidi[1], Shahab Falahi[2], Somayeh Farhang Dehghan[3], Homeira Ebrahimzadeh[4], Hori Ghaneialvar[5] & Rezvan Zendehdel[3]✉

The need to identify ammonia is necessary because of its harmful effects on the environment and humans. In this study, a colorimetric method was also developed for the detection of ammonia using silver nanoparticles (AgNPs) synthesized with the green approach. Biosynthesis of AgNPs was performed by silver nitrate as a silver precursor and *Smyrnium cordifolium* extract as a reducing and stabilizing agent. Plant extract was studied by FTIR and LC/Mass techniques. The optimization of the effective parameters was carried out with central composite design according to silver nitrate concentration, plant extract volume, pH, and temperature. Biosynthetic nano-silver was characterized with XRD, EDS/EDX, FE-SEM, FTIR, TGA, and DLS methods. The AgNPs was validated for ammonia colorimetric detection. Biosynthesis of AgNPs were increased in 20 mM $AgNO_3$, 5 ml *Smyrnium cordifolium* extract, pH 10, and the temperature of 70 °C. Crystal form of AgNPs characterized with XRD at 2Θ value of 38.34°, 44.19°, 64.74°, and 77.59° and spherical shape highlighted in the range between 77.8 and 93 nm. Plant extract consisted of polyphenol (phenolic acid, flavonoid, and terpenoid), fatty acid, amino acid, sugar, purine, and organic acid. AgNPs were used for colorimetric detection of ammonia by shifting the λmax from 580 to 490 nm. A method for ammonia detection was set up, with linear range of 0.5–200 ppm, detection limit of 0.028 ppm and recovery level of 96.3 ± 6.5%. In conclusion, a new biosynthetic method by specified local plant was developed to propose a simple and sensitive colorimetric method for soluble ammonia detection.

Keywords Green synthesis, Silver nanoparticles, *Smyrnium cordifolium*, Colorimetric method, Ammonia

Nanotechnology is a field with rapid growing. Nanoparticles is applicated in biotechnological, medical, and industrial purposes due to their unique physical and chemical properties[1]. Nano-silver particles specified with remarkable characteristics, such as conductivity and stability. These properties are applicable in various fields of catalysis, cosmetics, plastics, photonics, nanomedicine, food processing, biological tagging, biomedical imaging, and antimicrobial agent[2–4]. Silver nanoparticles (AgNPs) have attracted researchers in the field of colorimetry and spectroscopy due to their unique optical properties as well as their low cost compared to other nanoparticles of metals. These nanoparticles are able to strongly absorb and scatter visible light[5]. The optical properties of AgNPs are caused by the phenomenon of surface plasmon resonance (SPR)[6].

There are numerous methods for nanoparticles production such as biological approaches as well as physical and chemical syntheses. Physical and chemical methods are complex and expensive. In these days biosynthesis of nanoparticles is very attractive due to their simplicity, accessibility, affordability, safety to handle,

[1]Department of Occupational Health and Safety Engineering, School of Public Health and Safety, Shahid Beheshti University of Medical Sciences, Tehran, Iran. [2]Zoonotic Diseases Research Center, Ilam University of Medical Sciences, Ilam, Iran. [3]Department of Occupational Health and Safety Engineering, School of Public Health and Safety, Shahid Beheshti University of Medical Sciences, Tehran, Iran. [4]Department of Analytical Chemistry and Pollutants, Faculty of Chemistry and Petroleum Sciences, Shahid Beheshti University, Tehran, Iran. [5]Biotechnology and Medicinal Plants Research Center, Ilam University of Medical Sciences, Ilam, Iran. ✉email: Zendehdel76@Yahoo.com

and environmentally friendly characteristics[7,8]. Sahu and Kunjam synthesized AgNPs using bulb extract of *Urginea indica* (*Roxb*.). Silver nanoparticles had a spherical and cubic structure with particle size between 9 and 30 nm[9]. Asef et al. studied the bio-reduction method for fabricate silver nanoparticle production. In this study, silver nitrate and extract of *Moringa oleifera* leaves were employed as metallic precursor and reducing/capping agent, respectively. The characterization tests showed the successful synthesis of nanoparticles[10]. Kaur et al. were synthesizing silver nanoparticles with dried leaves of *Lycium shawii*. After the successful synthesis of nanoparticles, its microbial activities were also examined[11].

In this way, bioactive component of a plant extract perform reduction and stabilization of nanoparticles[12,13]. *Smyrnium cordifolium* Boiss (local name of *Vanegi*) is the only species of *Smyrnium* genus that has been reported in the flora of Iran[14]. The most important features of this plant include 80–120 cm in height, a thick and strong stem, greenish yellow flowers, and bright- green leaves[15]. *Smyrnium cordifolium* has medicinal properties and antioxidant activity. Limited information is available about this plant[15,16]. Based on the study of Tabaraki and Ghadiri[16], total phenolic content (TPC), total flavonoids content (TFC), and antioxidant activity of *Smyrnium cordifolium* extract is significant and impressive; Therefore, in our plan, this plant can reduce metal ions and synthesize metal nanoparticles.

Ammonia is a gas with distinct sharp scent[1], which is extensively used in a multitude of industries such as fertilizer production, creation of animal feed, manufacture of fibers and plastics, production of paper and pharmaceuticals, as well as in explosive manufacturing. Moreover, ammonium salts are employed as a cleansing agents and food additives. The solubility of ammonia and its salts in water and alcohol is remarkable[5,17]. These substances are very danger for aquatic species even in low concentrations[18]. Moreover, ammonia is a prominent soil contaminant with impact on the plants and aquatic animals[19]. Ammonia is reported as the irritant of eye, nose, throat, and skin. Furthermore, it was causes of vomiting, headaches, pneumonia, and death in research[20]. In this way, practical and simple determination of ammonia in aqueous samples is a serious need for environmental topics[21].

Various methods such as spectrometry[22], fluorescence[23], electrochemical[24], and ion chromatography[25] have been developed to identify ammonia. Very high sensitivity to changes in temperature and pH is the disadvantage of fluorescence method. Furthermore, this method is limited in detection range and is not proper in high concentrations[21]. Corrosion of the electrode, its stability and reliability, and the effect of environmental and interference compounds are known as drawbacks of the electrochemical detection method[21]. The most important problems of the ion chromatography method include the lack of selectivity in identifying ammonia, damage to the column, and the high cost of detection[26]. Spectrophotometric methods for ammonia determination are known as routine and common technique due to their wide application range and relative feasibility[27]. Several spectrophotometric methods have been used to detect dissolved ammonia in aqueous samples[21]. The most well-known techniques are the Nessler reaction and the Berthelot reaction[28]. Nessler reagent toxicity and unsuitable ammonia detection are an important hurdle of this technique[28]. Slow kinetics of Berthelot reaction is the disadvantage of method[1,28]. For detection of liquid ammonia, colorimetry method with SPR properties of metallic nanoparticles is an appropriate and useful approach due to its user-friendly, simplicity, high speed, low cost, and accuracy[29,30]. In these years colorimetric methods with green synthesis of metallic nanoparticles has evaluated for analyzing of ammonia in aqueous solution[30]. In the study of Dubas and Pimpan, AgNPs were synthesized by low-power UV source in the presence of poly methacrylic acid (PMA). Interaction between ammonia with AgNPs assessed by change from purple to yellow color. with detection limit of 5 ppm[31]. Ritthichai et al. synthetized AgNPs by silver nitrate as a silver precursor and tannic acid as a reducing agent. Detection limit of ammonia was evaluated 100 ppm[32] according to color change from orange-yellow to yellowish-green.

In the present study, a novel biosynthesis with a local plant was developed to evaluate ammonia concentration in aqueous samples.

Materials and methods

Chemicals

Ammonia (25%), Silver nitrate ($AgNO_3$, 99%), sodium hydroxide (caustic soda) (NaOH, 98%), hydrochloric acid (37%), iron nitrate ($Fe(NO_3)_3{\cdot}9H_2O$, 98%), copper sulfate ($CuSO_4{\cdot}5H_2O$, 99%), chromium nitrate ($Cr(NO_3)_3{\cdot}9H_2O$, 99.99%), cadmium sulfate ($3CdSO_4{\cdot}8H_2O$, 99.99%), manganese nitrate ($Mn(NO_3)_2$ 0.4 H_2O, 98%), nickel sulfate ($NiSO_4{\cdot}6H_2O$, 99%), mercury (II) nitrate ($Hg(NO_3)_2{\cdot}H_2O$, 99.99%) and ethanol (96%) were purchased from Merck (Germany).

Plant extract preparation

The plant of *Smyrnium cordifolium* Boiss was collected from Bankol mountain in Ivan City, Ilam province, Iran, during spring 2023. Voucher specimens was formally identified by Dr. Naser Abbasi, Head of Biotechnology and Medicinal Plants Research Center, Associate Professor of Pharmacology, School of Medicine, Ilam University of Medical sciences and deposited in the herbarium of Biotechnology and Medicinal Plants Research Center, Ilam University of Medical Sciences (Herbarium code: 1160). The plant collection process and other steps were performed in accordance with policies, guidelines, and legislation of International Union for Conservation of Nature and Iran Natural Resources and Watershed Management Organization. In this way, damage to the plant and species extinction do not occur. The aerial parts of plant washed with water and cut into smaller parts; dried at 30 °C and dark place for 7 days in free dust condition. After that dried samples were crushed to fine powder by an electric blender (350 A model, Gama Steel Co,. Iran)[33].

25 g of powder was extracted by Soxhlet method using a thimble filter. Soxhlet was performed for 3 h under ethanol and water mixture with 7:3 ratio by temperature program of 50 °C at 30 min and 150 min at 100 °C. To improve extraction of organic component such as flavonoid and phenolic acid from *Smyrnium cordifolium*

plant, ethanol-water mixture was used. However, low temperature for ethanol-water removing prevent structure change of the reducing compounds.

The extract mixture was filtered through a filter paper of Whatman No. 1. Plant extract concentrated by rotary evaporator device (RV 10 model, IKA Co,. Germany) for 3 h at 60 °C with the speed of 60 rpm (Fig. 1). Plant extract was stored in a refrigerator at 4 °C for further use[34].

The phytochemical composition of *Smyrnium cordifolium* extract was characterized using liquid chromatography- mass spectrometry (Alliance 2695 model, Waters Co,. USA) and Fourier transform infrared (FT-IR) spectroscopy (IFS 66 model, Bruker Co,. USA). A liquid chromatography- mass selective detector (LC-MS) was equipped with the autosampler and 5 µm, 4.6 µm × 150 mm, and C18 column. The mobile phase contains mixture A (Acetonitrile + 0.1% Formic Acid) and mixture B (H_2O + 0.1% Formic Acid) at a flow rate of 0.3 ml/min. The gradient conditions include 50% A and 50% B for 10 min and 80% A and 20% B between 10 and 25 min. Mass spectrometer consist of electrospray ionization (ESI) source which was used in positive and negative ionization mode. The capillary voltage was 4 kV, the desolvation temperature was set 350 °C and auxiliary gas with 200 L/h.

Green synthesis of AgNPs

To determine the most important parameters in the green synthesis of AgNPs, Design Expert Ver. 13 according to the central composite design (CCD) was used. In-dependent variables were $AgNO_3$ concentration, plant extract volume, pH, and temperature[34]. In this study for the biosynthesis reaction of 4 h $AgNO_3$ between 5 and 20 mM, plant extract volume in the range of 5–30 ml, pH between 4 and 10, and temperature from 35 to 70 °C entered to Design Expert software based on the previous studies[12,35,36]. However, UV-Vis Spectrometry absorbance (CE 2021 model, Agilent Co,. USA) at a wavelength of 580 nm was considered as the efficiency of AgNPs biosynthesis (Fig. 1). Determination of the optimal wavelength for AgNPs biosynthesis and UV-Vis absorption spectra are provided in the supplementary information, Fig. S1–S31.

As shown in Table 1 and 30 runs were proposed by the software while each variable was examined in 5 levels, including three main levels (– 1, 0, and + 1), two central points (+ α and – α), and three repetitions in the central point (full mode). After that the best model was determined using analysis of variance (ANOVA) test.

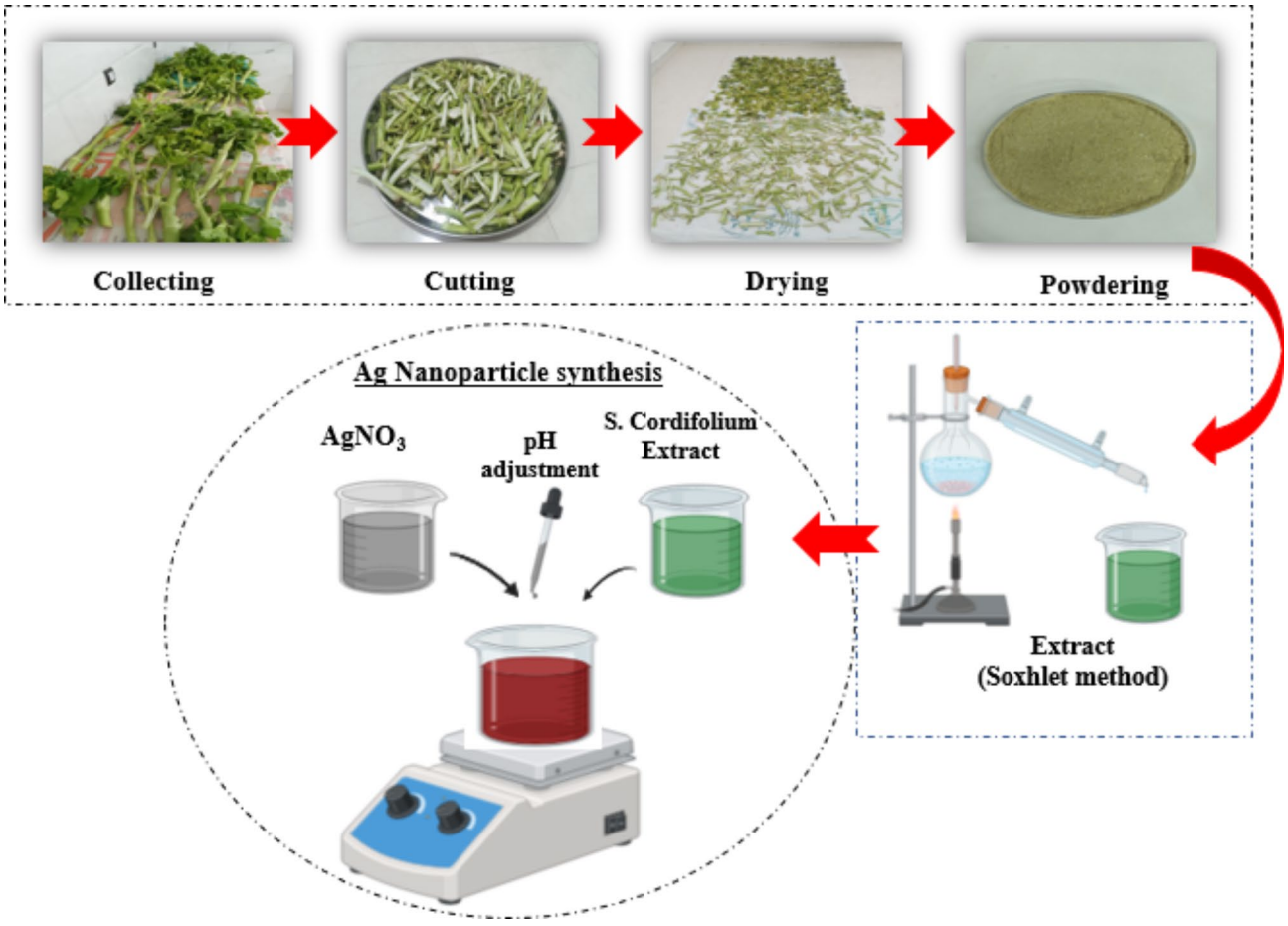

Fig. 1. Green synthesis of AgNPs.

	Independent variables				Response variable
Test No	$AgNO_3$ Concentration (mM)	Plant extract volume (mL)	PH	Temperature (ċ)	Absorbance
1	20	5	10	70	1.014
2	10.5	17.5	7	52.5	0.11
3	10.5	17.5	7	35	0.31
4	10.5	17.5	7	52.5	0.13
5	20	5	4	35	0.4
6	20	30	10	35	0.308
7	1	30	4	70	0.005
8	1	5	10	35	0.003
9	20	30	10	70	0.505
10	20	30	4	35	0.42
11	10.5	30	7	52.5	0.102
12	1	17.5	7	52.5	0.0033
13	10.5	17.5	7	52.5	0.12
14	10.5	17.5	7	52.5	0.198
15	1	5	4	35	0.001
16	1	5	10	70	0.037
17	1	30	10	35	0.0028
18	10.5	17.5	7	70	0.293
19	10.5	17.5	7	52.5	0.26
20	20	5	4	70	0.55
21	1	30	4	35	0.0025
22	20	17.5	7	52.5	0.463
23	1	30	10	70	0.0026
24	10.5	17.5	7	52.5	0.195
25	10.5	17.5	4	52.5	0.003
26	10.5	17.5	10	52.5	0.24
27	10.5	5	7	52.5	0.031
28	20	5	10	35	0.253
29	1	5	4	70	0.0021
30	20	30	4	70	0.1

Table 1. Design expert for AgNPs synthesis optimization.

Characterization of synthetized nanoparticles

Confirmation of AgNPs synthetize was performed by UV-Vis spectrophotometer (CE 2021 model, Agilent Co,. USA) and x-ray diffraction (XRD) (PW 1730 model, Philips Co,. Netherlands). XRD patterns was recorded with the operating power of 40 kV and 40 mA, and the diffraction data were collected between 10 and 80° (2θ). Field emission scanning electron microscope (FE-SEM) (Model: MIRA II and III model, Tescan Co,. Czech Republic) was employed to determine the particle size and morphology of AgNPs. Elemental character was assessed by energy dispersive x-ray spectroscopy (EDS/EDX) instrument. Chemical composition was studied by fourier transform infrared (FTIR) spectra (WQF-510 A) in 400–4000 cm^{-1}. The behavior stability was assessed through thermogravimetric analysis (TGA) (Q 600 model, TA CO,. USA). TGA was performed under a nitrogen atmosphere, temperature range 30–800 °C, and heating rate 10 °C/min. The average particle size and polydispersity index (PI) were determined by the dynamic light scattering (DLS) (SZ 100 model, Horiba CO,. Japan) at 25 °C with 90° detection angle.

Colorimetric detection of ammonia

Colorimetric reaction was prepared between 1 mL freshly synthetized AgNPs and 5 mL of ammonia standard solution. Standard solution of ammonia studied in the range of 0.5–200 ppm. Reaction efficiency was followed by UV-Vis spectrometry (Agilent, USA) at 490 nm.

Interference reaction was recorded with chemicals of Cr^{3+}, Fe^{3+}, Mn^{2+}, Cu^{2+}, Cd^{2+}, Ni^{2+}, and Hg^{2+12} in the presence of ammonia.

In addition, with the aim of application of this method in real samples, water samples were collected from agricultural water and the ammonia amount was determined by the colorimetric method developed by the present study.

Linear dynamic range (LDR), limit of detection (LOD), limit of quantification (LOQ), repeatability, and recovery were studied as validation parameters. Relative standard deviation (RSD) was applied as a repeatability based on the within-day and between-day assay via Eq. (1). Recovery parameter was determined through Eq. (2).

$$\text{RSD } (\%) = \frac{\text{Standard deviation}}{\text{Mean}} \times 100 \quad (1)$$

$$\text{Recovery } (\%) = \frac{\text{Measured Value}}{\text{Actual Value}} \times 100 \quad (2)$$

Results and discussion

Qualitative analysis of plant extract

Chemical profile of *Smyrnium cordifolium* extract based on the LC-Mass chromatogram was presented in Table 2; Fig. 2 for negative and positive ionization method.

Different components were characterized according to mass-to-charge ratio (m/z) map in the total ion chromatograms (TICs) and similarity with other reports.

There are 19 different compounds according to analysis of chromatogram and mass spectrum. These compounds categorized in 6 groups, including polyphenol, fatty acid, amino acid, sugar, purine, and organic acid. The polyphenol group contains three subgroups called phenolic acid, flavonoid, and terpenoid. Caffeic acid, sinapic acid hexose, quinic acid glucoside, and coumaric acid are in the phenolic acid. Quercetin hexoside, tricetin, gallocatechin, quercetin, and 6 methyl flavonol sodium salt compounds are in the flavonoid class and isorhamnetin 3-o-glucoside is in the terpenoid class. Two compounds of corchorifatty acid F and octadecanoic acid are in the fatty acid class and four compounds of asparagine, choline, phenyl alamine, and threanine are classified in the amino acid family. However, the compounds of D-cymarose, adenosine, and gluconic acid are in the sugar, purine, and organic acid family, respectively.

FTIR spectrum of *Smyrnium cordifolium* extract showed in Fig 3. The band of 3400 cm^{-1} corresponds to the hydroxyl groups stretching which is related to polyphenols and amino acids compounds[50–55]. The peak at 3375 and 3426 cm^{-1} corresponds to the N–H group stretching vibration in primary and secondary amines and amide compounds[35,56,57]. The observed peak at 1616 cm^{-1} belongs to the stretching vibration of the C=O group in carbonyl of amide[35,58].

In the study of Some et al., the biosynthesis of silver nanoparticle was performed by aqueous leaf extract of *Morus indica L. V1*. The phytochemicals identified in this extract included isoquercetin, sophoraisoflavanone A, cyclomorusin, mangiferin xanthonoid, gallic acid, kazinol B, and stigmasterol; However these compounds are in the flavonoid and phenolic groups[59].

Saad et al. identified 20 phytochemicals in pomegranate and watermelon wastes extracts. The main phenolic compounds for silver nanoparticle synthesis included quercetin, gallic acid, catechein, cyanidin-3-o-glu, punicalagin, ellagic acid, genistein, ferulic acid, and kampeferol[60].

Selim et al. shown that the phytochemicals of gallic acid, chlorogenic acid, caffeine, caffeic acid, syringic acid, rutin, ellagic acid, coumaric acid, vanillin, ferulic acid, naringenin, propyl gallate, quercetin, and cinnamic acid in extract of *deverra tortuosa* can produced nanoparticles of metals[61].

RT (min)	Product ion (m/z)	Compound	Class (Family)	Refs.
Negative mode				
2.69	179	Caffeic acid	Phenolic acid/ Polyphenol	37,38
4.45	385	Sinapic acid hexose	Phenolic acid/ Polyphenol	39
4.73	353	Quinic acid glucoside	Phenolic acid / Polyphenol	38
9.17	463	Quercetin hexoside	Flavonoid/ Polyphenol	40
9.81	477	Isorhamnetin 3-o-glucoside	Terpenoid/ Polyphenol	41
10.44	163	Coumaric acid	Phenolic acid/ Polyphenol	38
11.8	301	Tricetin	Flavonoid/ Polyphenol	40
12.13	328	Corchorifatty acid F	Fatty acid	42
12.61	329	Octadecanoic acid (Stearic acid)	Fatty acid	40
13.97	305	Gallocatechin	Flavonoid/ Polyphenol	43
Positive mode				
2.62	133	Asparagine	Amino acid	44
2.82	104	Choline	Amino acid	38,45
3.57	166	Phenyl alamine	Amino acid	38
4.35	120	Threanine	Amino acid	44
4.91	163	D-cymarose	Sugar	46
9.48	303	Quercetin	Flavonoid/ Polyphenol	47
9.79	268	Adenosine	Purine	45,48
16.41	235	Gluconic acid	Organic acid	49
19.51	274	6 Methyl flavonol sodium salt	Flavonoid/ Polyphenol	47

Table 2. Compounds of *Smyrnium cordifolium* extract determined by LC-Mass.

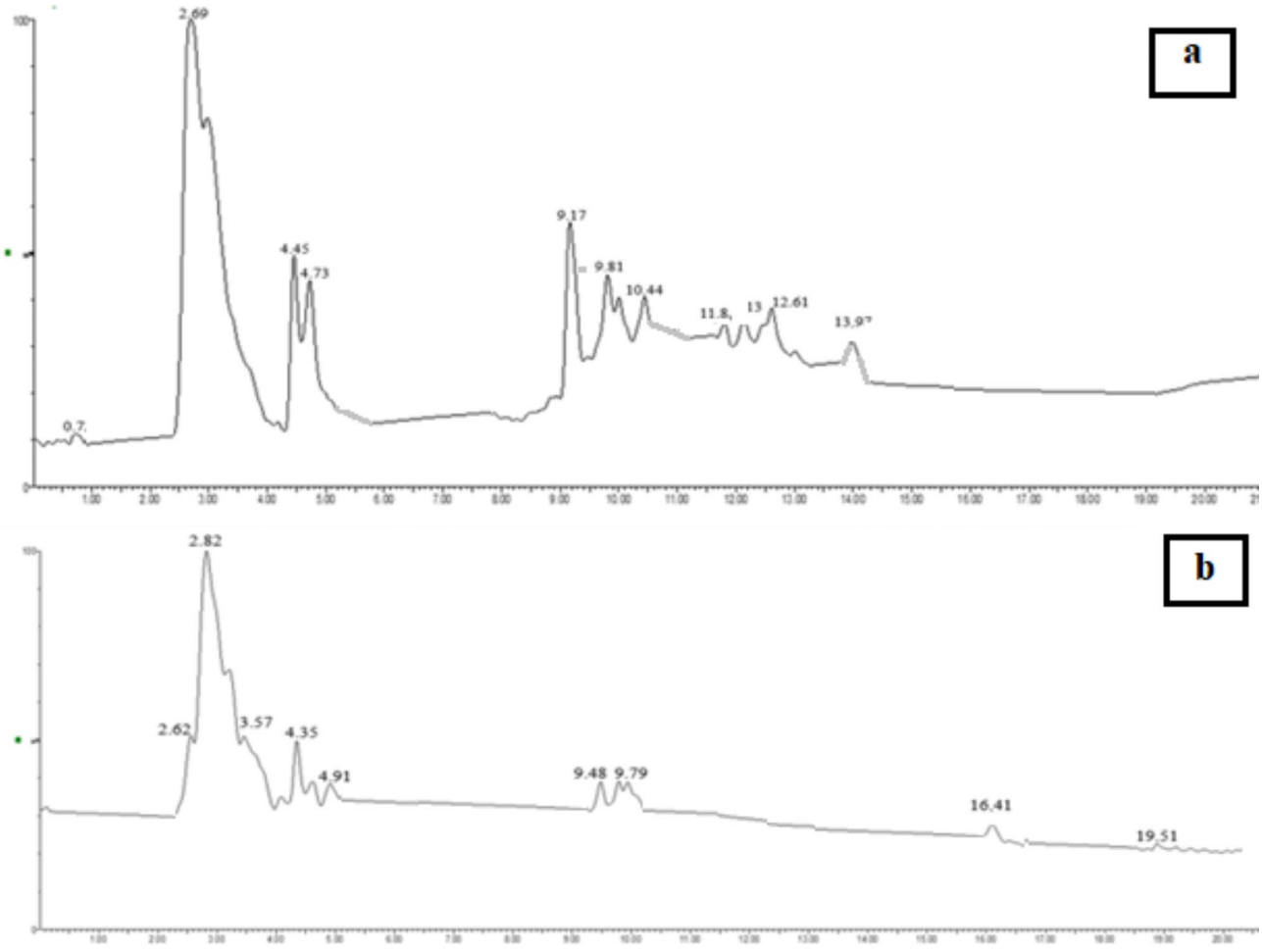

Fig. 2. Mass chromatograms (TICs) of *Smyrnium cordifolium* extract. (**a** Negative mode and **b** positive mode)

Presence of chemicals such as phenolic acid, flavonoid, and terpenoid groups in *Smyrnium cordifolium* highlighted the reduction properties of plant extract which used for synthetizing, capping, and stabilization of silver nanoparticles.

Green synthesis of AgNPs

Green chemistry is a new approach for nanoparticle synthesis which is overcome the problems of physical and chemical methods. The major feature of this method is simplicity in synthesis, cost-effectiveness, and environment friendly approach[62]. Application of plants in this marathon has advantages of availability, fewer biohazards, user safety, and inexpensive[63]. Plant extract with several bioactive phytochemicals such as phenolic acid, flavonoid, alkaloids, ketones, aldehydes, tannins, terpenoids, organic acids, and proteins can interact with silver ions to reduce and stabilize the AgNPs[13,59]. The *Smyrnium cordifolium* located in Ilam province, Iran, is one of the natural and self-growing plants, which has abundant bioactive compounds and secondary metabolites. Therefore, in this study, for the first time, it was planning to use *Smyrnium cordifolium* extract for reducing of silver ions as well as stabilizing agent of AgNPs.

Finding of CCD model showed the quadratic function is an appropriate model to fit dependent variables and solution absorbance (Eq. 3).

$$\begin{aligned}\text{Absorbance} = {} & +0.1640 + 0.2562A + 0.0884B + 0.0794C + 0.0786D - 0.2055AB - 0.1226BD \\ & + 0.1344CD - 0.1039B^2 + 0.1311D^2; \text{A:AgNO3 Concentration, B:Plant extract volume, C:pH, D:Temperature}\end{aligned} \quad (3)$$

The results of the ANOVA test are shown in Table 3. The *P*-value of model was significant ($p < 0.0001$), lack-of-fit was not significant ($p = 0.3917$), and F-value is enough large (29.55). Moreover, regression of coefficient (R^2) was 0.87 as a suitable fitting marker between independent parameters ($AgNO_3$ concentration, plant extract volume, pH, and temperature) and response variable. The difference less than 0.2% between adjusted R^2 and predicted R^2 also shows good prediction of model. Adeq precision higher than 4 highlighted its acceptability and desirability due to appropriate signal to noise factor. In this way optimum conditions of AgNPs biosynthesis with *Smyrnium cordifolium* were 20 mM $AgNO_3$, 5 ml *Smyrnium cordifolium* extract, pH = 10, and temperature of 70 °C.

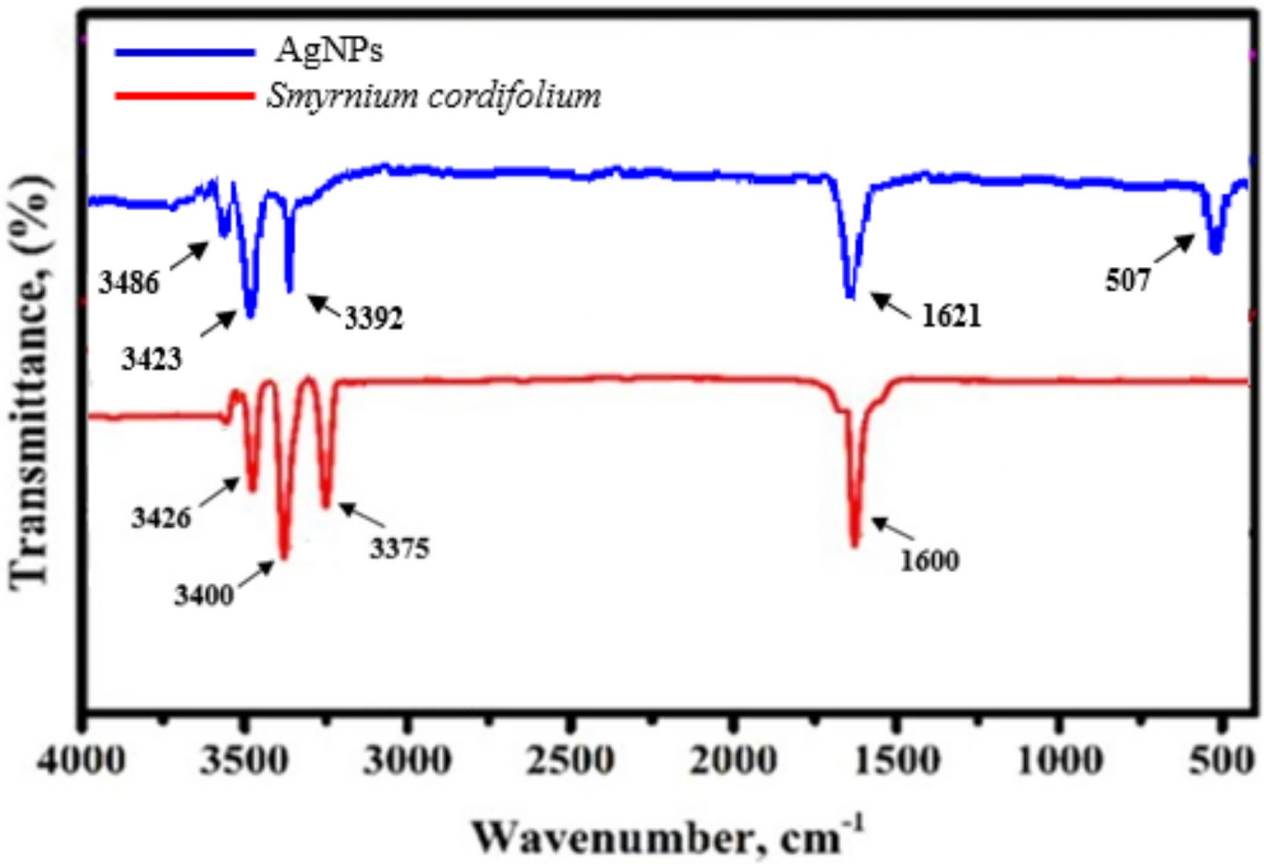

Fig. 3. FTIR of *Smyrnium cordifolium* extract and AgNPs.

The interaction between $AgNO_3$ concentration and plant extract volume show increasing of AgNPs formation in higher $AgNO_3$ concentration (Fig. 4). It could be related to higher positive charge and growing the reduction rate[35,64]. However, three-dimensional response between temperature and pH presented increasing of AgNPs synthetize in higher temperature and alkaline pH (Fig. 4). At higher temperatures, a speed of the reaction improved due to the facilitate of free electrons movement[12,65]. Hydroxyl ions in alkaline pH, increase the reduction of silver metal. Alkaline condition leads to an intermediate reaction and Ag_2O production (Eq. 4). In this way, Ag_2O precipitation act as a nucleus of AgNPs growing[66,67].

$$2Ag^{+} + 2OH^{-} \leftrightarrow Ag_2O + H_2O \quad (4)$$

AgNPs characterization

Synthesis of AgNPs was confirmed by color change from colorless to dark orange (Fig. 5). Moreover, the visible assessment of AgNPs shows maximum absorption at 580 nm. In other words, UV–Vis analysis shows that absorption in plant extract of 360 nm wavelength shifted to 580 nm wavelength by adding silver nitrate and finally forming silver nanoparticles. (Fig. 6a). Recently UV–Vis spectroscopy was reported as an indirect way for recognition of the nanoparticles formation[68,69]. Electron excitation in the surface of nanoparticles caused absorption band conduction which is named SPR. Therefore, color change and the red shift signal with the increase in absorption level at 580 nm confirmed the reduction of silver ion (Ag^+) to silver metal (Ag^0) due to SPR property[70,71]. Biosynthesis of silver nanoparticles is published by wavelength change in the range of 400–580 nm[30,51,72,73]. In this way size and shape of metal nanoparticles is related to specific UV-Vis absorption[13,74]. However, biosynthesize of AgNPs with *Smyrnium cordifolium* extract is developed due to specific vibration band determined by spectrometer.

XRD patterns of AgNPs were shown in Fig. 6b. Existence of well-shaped peaks at 2Θ value of 38.34°, 44.19°, 64.74°, and 77.59° (111, 200, 220, 311 crystal planes) demonstrated the formation of the crystal form of AgNPs[73,75].

Elemental composition of AgNPs was presented with energy dispersive X-ray spectroscopy EDS in Fig. 6c. The highest signal of 3KV (1,23) confirmed the production of AgNPs from silver ion through *Smyrnium cordifolium*[1,35].

The weight% of elements including silver (Ag), carbon (C), chlorine (Cl), and oxygen (O) are 77.29%, 18.17%, 2.64%, and 1.91%, respectively. However, the weak signals of C, Cl, and O are attributed to the capping agent and

Functions from modeling					
Source	**Sequential *p*-value**	**Lack of Fit *p*-value**	**Adjusted R^2**	**Predicted R^2**	
Linear	0.0017	0.0097	0.5110	0.1595	
2FI	0.0031	0.0796	0.8268	0.4685	
Quadratic	**< 0.0001**	**0.3917**	**0.9211**	**0.8295**	**Suggested**
Cubic	0.4103		0.9345		**Aliased**
Summary of ANOVA					
Source	**Sum of squares**	**Mean square**	**F-value**	***P*-value**	
Model	1.10	0.1225	29.55	< 0.0001	**Significant**
A	0.4521	0.4521	109.09	< 0.0001	
B	0.0477	0.0477	11.51	0.0048	
C	0.0652	0.0652	15.75	0.0016	
D	0.0642	0.0642	15.50	0.0017	
AB	0.2117	0.2117	51.08	< 0.0001	
BD	0.1256	0.1256	30.31	0.0001	
CD	0.1508	0.1508	36.39	< 0.0001	
B^2	0.0343	0.0343	8.29	0.0129	
D^2	0.0546	0.0546	13.18	0.0031	
Residual	0.0539	0.0041			
Lack of Fit	0.0367	0.0046	1.33	0.3917	**Not significant**
Pure Error	0.0172	0.0034			
Cor Total	1.16				
Regression coefficients					
R^2 = 0.9534	Adjusted R^2 = 0.9211	Predicted R^2 = 0.8295	Adeq Precision = 23.7550		

Table 3. Output of ANOVA tests for AgNPs biosynthesis. 2FI: two-factor interaction, A: AgNO3 Concentration, B: Plant Extract volume, C: pH, D: Temperature. Significant values are in bold.

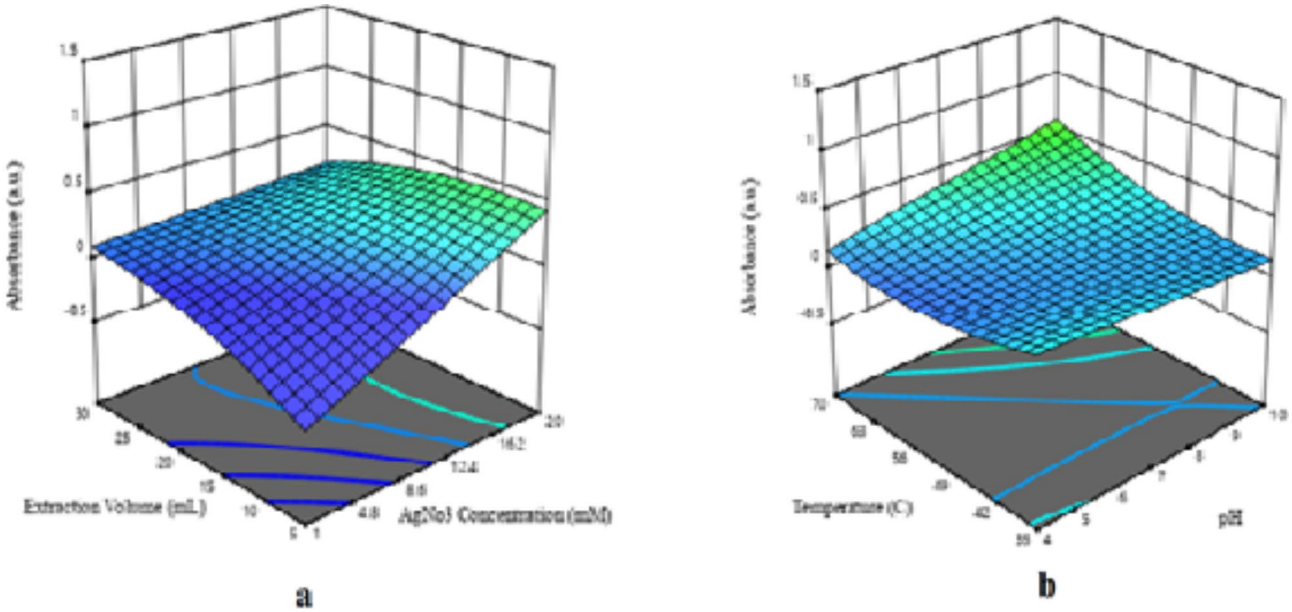

Fig. 4. Three-dimensional response AgNPs biosynthesis (**a** Plant extract volume and $AgNO_3$ Concentration, **b** Temperature and pH).

bioactive compounds of the plant extract[51,76]. Surface morphology of AgNPs is shown in Fig. 6d according to the FE-SEM image. Synthetized AgNPs is spherical with the size range between 77.8 and 93 nm.

In the FTIR spectra of AgNPs (Fig. 3), four bands of the *Smyrnium cordifolium* extract with a slight shift were found at 3486, 3423, 3392, and 1621 cm^{-1}. There was a new peak at 507 cm^{-1}, which indicates the oxygen-metal band (O–Ag) and confirms the successful synthesis of AgNPs[12,35,73].

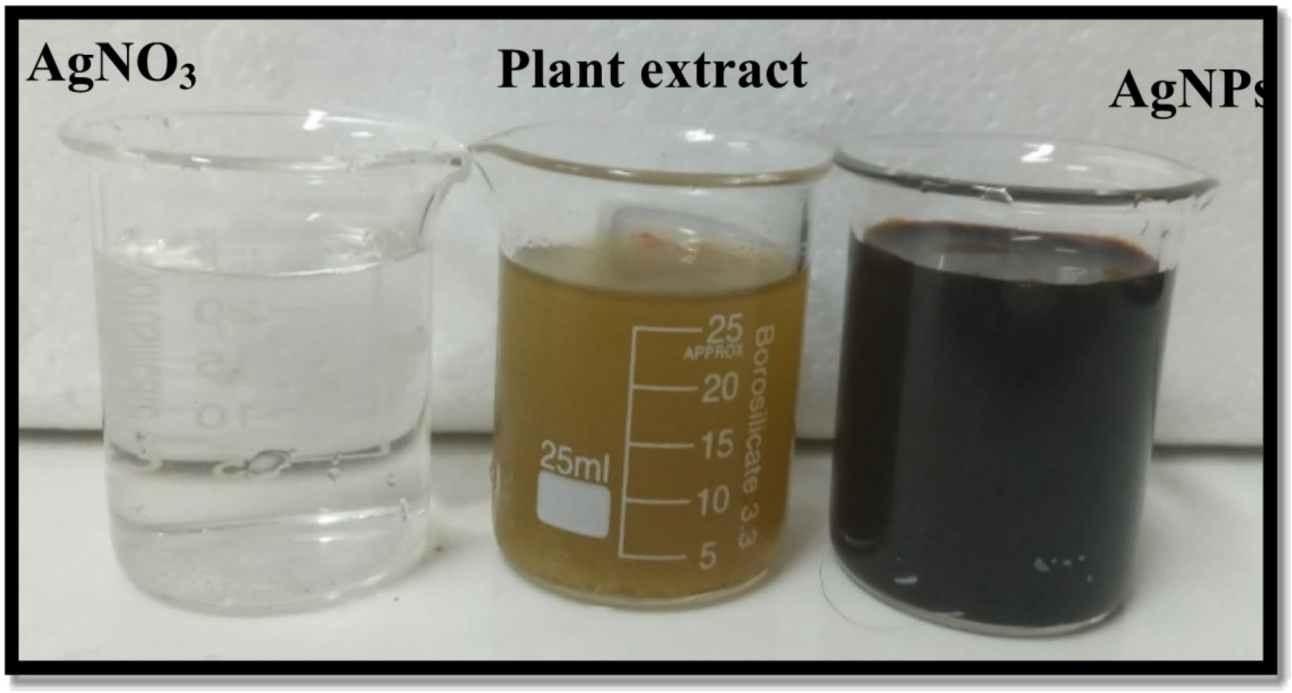

Fig. 5. Color change in AgNPs production.

As shown in Fig. 6e, TGA of AgNPs presented the slight weight loss at 100 °C which is related to water absorbed on the surface of AgNPs. Significant weight loss was observed in the TGA curve prior to 690 °C, attributed to the destruction and removal of phytochemicals and stabilizing agents on the surface of AgNPs. However, total weight loss of AgNPs is 12.82 as the same as other studies[35,77,78]. Hydrodynamic size of AgNPs is 473.5 nm with PI value of 0.615 (Fig. 6f) based on the DLS test. AgNPs with a PI value less than 0.7 indicates the synthesis of silver nanoparticle with suitable quality, relatively proper defined dimensions, and high monodispersity[51].

Silver nanoparticle synthesized from *Smyrnium cordifolium* extract have suitable thermal stability. Phytochemicals and bioactive compounds in *Smyrnium cordifolium* extract are responsible as a stability and capping agents of silver nanoparticles.

Colorimetric detection of ammonia

The interaction between synthetized AgNPs and ammonia solution clarified by color change of mixture from dark orange to amber. This color conversion is related to blue shift of maximum wavelength from 580 to 490 nm (Fig. 6a). According to other studies[18,35] surface charge of silver AgNPs increases by ammonia solution according to silver diamine complex $[Ag(NH_3)_2]^+$ formation which is presented by blue shift of wavelength from 580 to 490 nm. This reaction decreases the amount of AgNPs which it shows significant change in SPR band. However, dielectric constant of the mixture and the distance between the particles is changed[12,35]. Color change of AgNPs and ammonia interaction is related to ammonia concentration and was studied by UV-Vis spectroscopy as the method of ammonia detection.

Advised method for assessment of ammonia was carried out by adding 1 mL synthetized AgNPs and 5 mL of ammonia solution. The blue shift of wavelength from 580 to 490 nm highlighted absorption spectra for the detection of ammonia. Validation parameters are presented in Table 4.

The regression of the calibration curve was $\geq 99.76\%$, and ammonia recovery values were $96.3 \pm 6.5\%$.

The selectivity of suggested method was tested using potential interfering cation species in solution. As shown in Fig. 7, There is any amber color for cation interferences with AgNPs due to suitable selectivity of suggested method.

Feasibility of ammonia assessment was evaluated in environmental applications using agricultural irrigation sampling. Seven water samples were selected from two stations.

The ammonia concentration in a real sample was presented between 2.1 and 3.3 ppm (Table 5). Moreover, by adding 100 ppm of standard solution in all samples, recovery of method was calculated in the range of 98.8–104%.

we compared the colorimetric method of ammonia detection according to *Smyrnium Cordifolium* bio-synthesized AgNPs with other plant extract in Table 6. In two studies by Ismail et al., silver nanoparticles were successfully synthesized using extracts of *Convolvulus Cneorum* and *Durenta erecta*[12,35].Ammonia detection were not validated by accuracy and precision tests in these studies. Jongprakobkit et al. developed a colorimetric method for ammonia detection by anthocyanins from *red cabbage*. The detection limit and linear range of this method were obtained as 0.29 and 1–25 ppm, respectively[79]. It seems that the linear range of this study is small, and it covers a lower concentration range of ammonia than our study. In the study by Alzahrani, silver nanoparticles

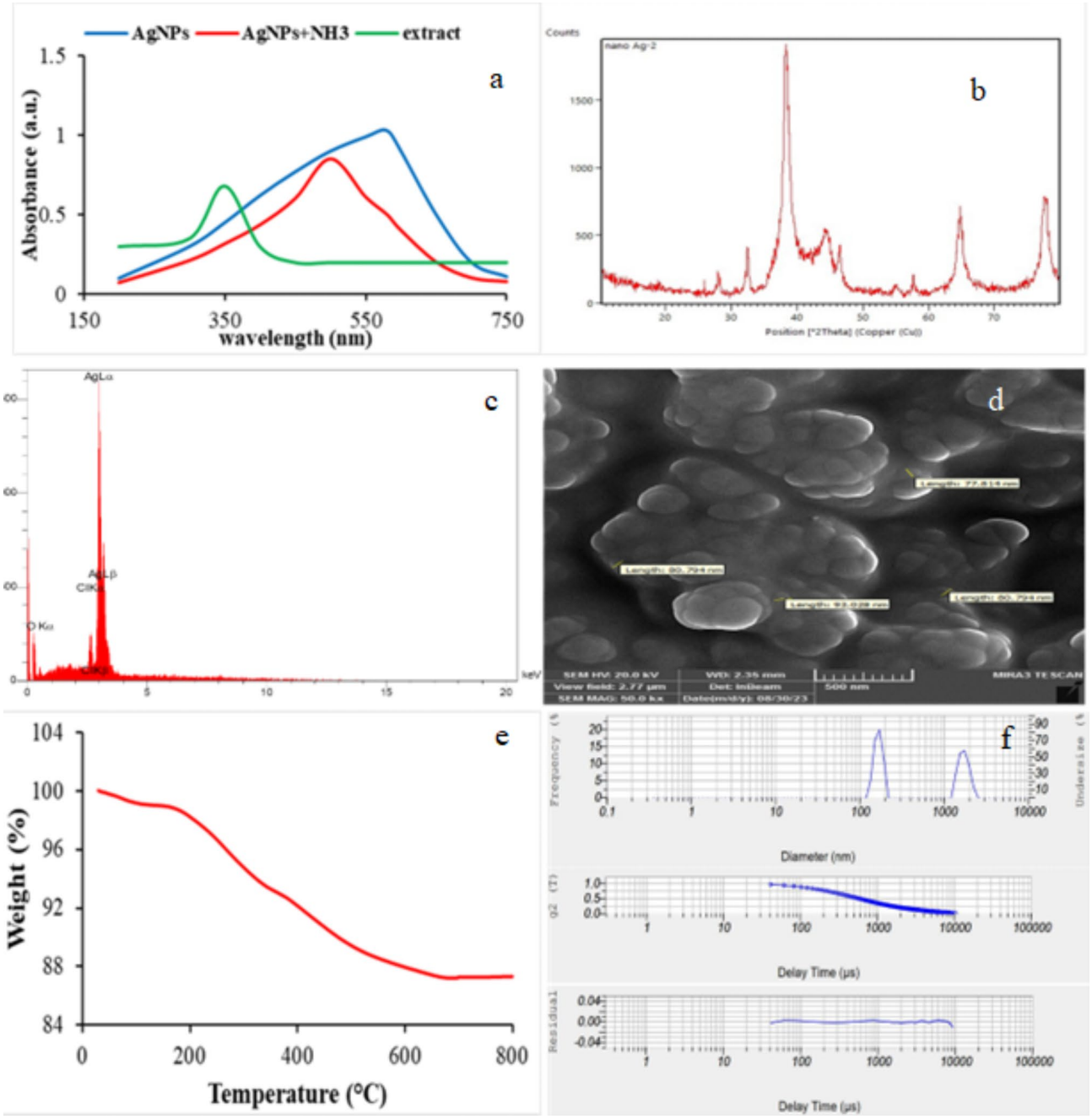

Fig. 6. Characterization AgNPs (**a** UV-Vis, **b** XRD, **c** EDS, **d** FE-SEM, **e** TGA, **f** DLS).

Linear range (ppm)	LOD (ppm)	LOQ (ppm)	Calibration curve	RSD% range ($n=3$)
				Within day between day
0.5–200	0.028	0.084	Y = 0.0001x + 0.5304	2.83–4.73 3.46–4.96

Table 4. Method validation of ammonia detection.

synthesized from *Durian* fruit shell. However, Srikhao et al., studied green method through *sugarcane* plant extract[30].They missed some validation parameters such as relative standard deviation as precision tests. We evaluate all of analysis validation parameters while the results show validation parameters of our method are better or comparable with the results of other.

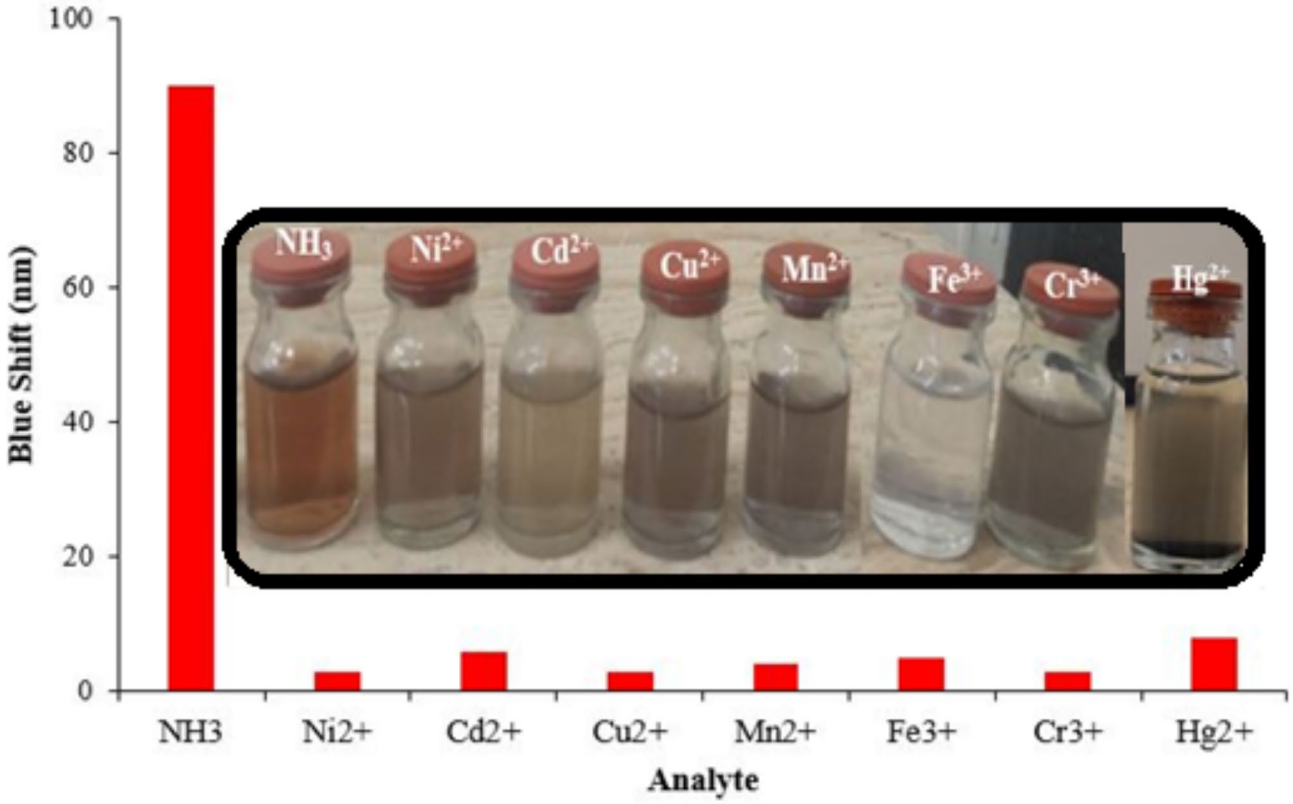

Fig. 7. Selectivity test of ammonia determination.

Sample	Measured amount (ppm)	Recovery (%)
1	2.27	99.6
2	2.1	98.8
3	2.93	101
4	2.6	104
5	2.8	99.8
6	3.3	102.5
7	3	100.2

Table 5. Determination of ammonia in real samples

Conclusions

In this study, silver nanoparticles were used for colorimetric assessment of ammonia solution. AgNPs were synthetized according to green chemistry approach by *Smyrnium cordifolium* extract. However, reduction potency of Iranian local Smyrnium *cordifolium* were highlighted by 19 different chemicals. Bio-synthetize was optimized with CCD in 20 mM $AgNO_3$, 5 ml *Smyrnium cordifolium* extract, pH 10, and temperature of 70 °C. An environmentally friendly method was validated for the assessment of agricultural irrigation samples. In conclusion suggested reactions including bio-synthesize and silver-ammonia interaction are simple, sensitive, inexpensive, and reproducible which are comparable with other reports.

Nanoparticles (NPs)	Green source	Matrix	LDR (ppm)	LOD (ppm)	RSD (%)	Recovery (%)	Refs.
Ag NPs	*Convolvulus cneorum* (*C. cneorum*)/Plant	Aqueous solution	5-300	5	–	–	12
Ag NPs	*Durenta erecta* (D. erecta)/Plant	Aqueous solution	5-100	0.5	–	–	35
Anthocyanin	*Red cabbage*/plant	Water	1–25	0.29	1.7–9.8	89.6– 110.5	79
Ag NPs	*Durian*/plant	Aqueous solution marine and bottled waters	500–3000	–	–	89.66–101.44	18
Ag NPs	*Sugarcane*/plant	Aqueous solution and environmental water	0–50	5	–	–	30
Ag NPs	*Smyrnium cordifolium*/ plant	Aqueous solution and water	0.5–200	0.028	2.83–4.96	96.3 ± 6.5	This study

Table 6. Comparison of the ammonia detection with different plant extract. *Ag NPs* silver nanoparticles, *LOD* limit of detection, *LDR* linear dynamic range, *RSD* relative standard deviation.

Data availability

All data used were published in this manuscript and can be requested from the corresponding author.

Received: 28 March 2024; Accepted: 12 September 2024
Published online: 15 October 2024

References

1. Tomer, A. K., Rahi, T., Neelam, D. K. & Dadheech, P. K. Cyanobacterial extract-mediated synthesis of silver nanoparticles and their application in ammonia sensing. *Int. Microbiol.* **22**, 49–58 (2019).
2. Pandey, S. & Nanda, K. K. Au nanocomposite based chemiresistive ammonia sensor for health monitoring. *Acs Sens.* **1**, 55–62 (2016).
3. Pandey, S. & Ramontja, J. Rapid, facile microwave-assisted synthesis of xanthan gum grafted polyaniline for chemical sensor. *Int. J. Biol. Macromol.* **89**, 89–98 (2016).
4. Pandey, S., Goswami, G. K. & Nanda, K. K. Green synthesis of polysaccharide/gold nanoparticle nanocomposite: an efficient ammonia sensor. *Carbohydr. Polym.* **94**, 229–234 (2013).
5. Edison, T. N. J. I., Atchudan, R. & Lee, Y. R. Optical sensor for dissolved ammonia through the green synthesis of silver nanoparticles by fruit extract of Terminalia chebula. *J. Cluster Sci.* **27**, 683–690 (2016).
6. Amirjani, A. & Fatmehsari, D. H. Colorimetric detection of ammonia using smartphones based on localized surface plasmon resonance of silver nanoparticles. *Talanta*. **176**, 242–246 (2018).
7. Abbasi, Z., Feizi, S., Taghipour, E. & Ghadam, P. Green synthesis of silver nanoparticles using aqueous extract of dried Juglans regia green husk and examination of its biological properties. *Green. Process. Synthesis*. **6**, 477–485 (2017).
8. Gul, S. et al. Novel synthesis of silver nanoparticles using melon aqueous extract and evaluation of their feeding deterrent activity against housefly Musca domestica. *Asian Pac. J. Trop. Disease*. **6**, 311–316 (2016).
9. Sahu, U. & Kunjam, S. Green Synthesis and Characterization of Silver (Ag) Nanoparticles from Aqueous Bulb Extract of Urginea Indica (Roxb.) Kunth and its Antimicrobial Activity. *Available at SSRN 4809271*.
10. Asif, M. et al. Green synthesis of silver nanoparticles (AgNPs), structural characterization, and their antibacterial potential. *Dose-Response*. **20**, 15593258221088709 (2022).
11. Kaur, N. et al. Lycium Shawii mediated green synthesis of silver nanoparticles, characterization and assessments of their phytochemical, antioxidant, antimicrobial properties. *Inorg. Chem. Commun.* **159**, 111735 (2024).
12. Ismail, M. et al. Phytosynthesis of silver nanoparticles; naked eye cellulose filter paper dual mechanism sensor for mercury ions and ammonia in aqueous solution. *J. Mater. Sci.: Mater. Electron.* **30**, 7367–7383 (2019).
13. Rashidi, M. A. et al. The emerging potential of green-synthesized nanoparticles as colorimetric sensors for ammonia detection. *Microchem. J.*, 109646 (2023).
14. Amiri, H., Khavari-Nejad, R. A., Masoud, S., Chalabian, F. & Rustaiyan, A. Composition and antimicrobial activity of the essential oil from stems, leaves, fruits and roots of Smyrnium cordifolium Boiss. From Iran. *J. Essent. Oil Res.* **18**, 574–577 (2006).
15. Doodman, S., Saeidi, K., Lorigooini, Z. & Kiani, M. Jamshidi-kia, F. Phytochemistry and pharmacological effects of Smyrnium cordifolium Boiss.(Apiaceae): a review. *Adv. Herb. Med.* **5**, 49–56 (2019).
16. Tabaraki, R. & Ghadiri, F. In vitro antioxidant activities of aqueous and methanolic extracts of Smyrnium cordifolium Boiss and Sinapis arvensis L. *Int. Food Res. J.* **20** (2013).
17. Nuñez, L., Cetó, X., Pividori, M. I., Zanoni, M. V. B. & Del Valle, M. Development and application of an electronic tongue for detection and monitoring of nitrate, nitrite and ammonium levels in waters. *Microchem. J.* **110**, 273–279 (2013).
18. Alzahrani, E. Colorimetric detection of ammonia using synthesized silver nanoparticles from durian fruit shell. *J. Chem.* **2020**, 1–11 (2020).
19. Srivastava, V. & Jain, K. Mechanism of enhancement in NH 3 sensing for surface functionalized WO 3 film. *RSC Adv.* **5**, 56993–56997 (2015).
20. Wetchakun, K. et al. Semiconducting metal oxides as sensors for environmentally hazardous gases. *Sens. Actuators B*. **160**, 580–591 (2011).
21. Li, D., Xu, X., Li, Z., Wang, T. & Wang, C. Detection methods of ammonia nitrogen in water: a review. *TRAC Trends Anal. Chem.* **127**, 115890 (2020).
22. Zhou, H., Song, Y. & Yang, Z. A reversible spectrophotometric method based on a coupled microfluidic chip for highly selective ammonium detection. *J. Chem.* **2019**, 1–8 (2019).
23. Zhu, Y. et al. Development and application of a portable fluorescence detector for shipboard analysis of ammonium in estuarine and coastal waters. *Anal. Methods*. **10**, 1781–1787 (2018).
24. Choosang, J. et al. Simultaneous detection of ammonium and nitrate in environmental samples using on ion-selective electrode and comparison with portable colorimetric assays. *Sensors*. **18**, 3555 (2018).
25. Wang, P. Y., Wu, J. Y., Chen, H. J., Lin, T. Y. & Wu, C. H. Purge-and-trap ion chromatography for the determination of trace ammonium ion in high-salinity water samples. *J. Chromatogr. A*. **1188**, 69–74 (2008).
26. Xia, L., Qing, X., Yafei, G., Xiaoping, Y. & Tianlong, D. in *International Conference on Biological Engineering and Pharmacy 2016 (BEP* 339–341 (Atlantis Press). (2016).

27. Lin, K., Zhu, Y., Zhang, Y. & Lin, H. Determination of ammonia nitrogen in natural waters: recent advances and applications. *Trends Environ. Anal. Chem.* **24**, e00073 (2019).
28. Timmer, B., Olthuis, W. & Van Den Berg, A. Ammonia sensors and their applications—a review. *Sens. Actuators B.* **107**, 666–677 (2005).
29. Dayanidhi, K., Vadivel, P. & Noorjahan, S. Colorimetric detection of ammonia and hydrogen peroxide in aqueous solutions using green synthesized silver nanoparticles from soapberry pericarps. (2023).
30. Srikhao, N., Kasemsiri, P., Lorwanishpaisarn, N. & Okhawilai, M. Green synthesis of silver nanoparticles using sugarcane leaves extract for colorimetric detection of ammonia and hydrogen peroxide. *Res. Chem. Intermed.* **47**, 1269–1283 (2021).
31. Dubas, S. T. & Pimpan, V. Green synthesis of silver nanoparticles for ammonia sensing. *Talanta*. **76**, 29–33 (2008).
32. Ritthichai, T. & Pimpan, V. Ammonia sensing of silver nanoparticles synthesized using tannic acid combined with UV radiation: Effect of UV exposure time. *J. King Saud University-Science*. **31**, 277–284 (2019).
33. Nazari, P., Yaghmaei, P., Rangin, A. & Abbasi, N. Influence of Smyrnium cordifolium Boiss extract on the hippocampus Mu-opioid receptors in mice. *J. Basic. Res. Med. Sci.* **7**, 29–37 (2020).
34. Nazari, P., Yaghmaei, P., Rangin, A. & Abbasi, N. Effects of curzerene and Smyrnium cordifolium Boiss. Extract on addiction withdrawal syndrome in mice. *J. Herbmed Pharmacol.* **7**, 280–286 (2018).
35. Ismail, M. et al. Biosynthesis of silver nanoparticles: a colorimetric optical sensor for detection of hexavalent chromium and ammonia in aqueous solution. *Phys. E: Low-dimensional Syst. Nanostruct.* **103**, 367–376 (2018).
36. Traiwatcharanon, P., Timsorn, K. & Wongchoosuk, C. Effect of pH on the green synthesis of silver nanoparticles through reduction with pistiastratiotes l. extract. *Adv. Mater. Res.* **1131**, 223–226 (2016).
37. El Sayed, A. M., Basam, S. M., El-Naggar, E. M. A., Marzouk, H. S. & El-Hawary LC–MS/MS and GC–MS profiling as well as the antimicrobial effect of leaves of selected Yucca species introduced to Egypt. *Sci. Rep.* **10**, 17778 (2020).
38. Nemzer, B., Abshiru, N. & Al-Taher, F. Identification of phytochemical compounds in coffea arabica whole coffee cherries and their extracts by LC-MS/MS. *J. Agric. Food Chem.* **69**, 3430–3438 (2021).
39. Bystrom, L. M., Lewis, B. A., Brown, D. L., Rodriguez, E. & Obendorf, R. L. Characterisation of phenolics by LC–UV/Vis, LC–MS/MS and sugars by GC in Melicoccus bijugatus Jacq.'Montgomery'fruits. *Food Chem.* **111**, 1017–1024 (2008).
40. Kang, J., Price, W. E., Ashton, J., Tapsell, L. C. & Johnson, S. Identification and characterization of phenolic compounds in hydromethanolic extracts of sorghum wholegrains by LC-ESI-MSn. *Food Chem.* **211**, 215–226 (2016).
41. Khallouki, F., Ricarte, I., Breuer, A. & Owen, R. W. Characterization of phenolic compounds in mature Moroccan medjool date palm fruits (Phoenix dactylifera) by HPLC-DAD-ESI-MS. *J. Food Compos. Anal.* **70**, 63–71 (2018).
42. Teoh, W. Y. et al. LC-MS/MS and GC-MS analysis for the identification of bioactive metabolites responsible for the antioxidant and antibacterial activities of Lygodium microphyllum (cav.) R. Br. *Separations*. **10**, 215 (2023).
43. Fracassetti, D., Costa, C., Moulay, L. & Tomás-Barberán, F. A. Ellagic acid derivatives, ellagitannins, proanthocyanidins and other phenolics, vitamin C and antioxidant capacity of two powder products from camu-camu fruit (Myrciaria dubia). *Food Chem.* **139**, 578–588 (2013).
44. Molina-Calle, M., Priego-Capote, F. & de Castro, M. L. Characterization of Stevia leaves by LC–QTOF MS/MS analysis of polar and non-polar extracts. *Food Chem.* **219**, 329–338 (2017).
45. Vigh, S. et al. Analysis of phytoconstituent profile of fenugreek–Trigonella foenuem-graecum L.-seed extracts. *Studia Univ. Babes-Bolyai Chem.* **62**, 145–166 (2017).
46. Tapfuma, K. I., Mekuto, L., Makatini, M. M. & Mavumengwana, V. The LC-QTOF-MS/MS analysis data of detected metabolites from the crude extract of Datura stramonium leaves. *Data Brief.* **25**, 104094 (2019).
47. Kaur, J., Dhiman, V., Bhadada, S., Katare, O. & Ghoshal, G. LC/MS guided identification of metabolites of different extracts of Cissus quadrangularis. *Food Chem. Adv.* **1**, 100084 (2022).
48. Chen, S., Liu, J. Q., Xiao, H., Zhang, J. & Liu, A. Simultaneous qualitative assessment and quantitative analysis of metabolites (phenolics, nucleosides and amino acids) from the roots of fresh Gastrodia elata using UPLC-ESI-Triple quadrupole ion MS and ESI-linear ion trap high-resolution MS. *Plos One*. **11**, e0150647 (2016).
49. Felipe, D. F., Brambilla, L. Z., Porto, C., Pilau, E. J. & Cortez, D. A. Phytochemical analysis of Pfaffia glomerata inflorescences by LC-ESI-MS/MS. *Molecules*. **19**, 15720–15734 (2014).
50. Mohammed, A. A. et al. Antioxidant and antibacterial activities of silver nanoparticles biosynthesized by Moringa Oleifera through response surface methodology. *Journal of Nanomaterials* 1–15 (2022). (2022).
51. Khane, Y. et al. Green synthesis of silver nanoparticles using aqueous Citrus limon zest extract: characterization and evaluation of their antioxidant and antimicrobial properties. *Nanomaterials*. **12**, 2013 (2022).
52. Nguyen, T. T. N. et al. Silver and gold nanoparticles biosynthesized by aqueous extract of burdock root, Arctium lappa as antimicrobial agent and catalyst for degradation of pollutants. *Environ. Sci. Pollut. Res.* **25**, 34247–34261 (2018).
53. Kadam, J., Dhawal, P., Barve, S. & Kakodkar, S. Green synthesis of silver nanoparticles using cauliflower waste and their multifaceted applications in photocatalytic degradation of methylene blue dye and hg 2 + biosensing. *SN Appl. Sci.* **2**, 1–16 (2020).
54. Yassin, M. T., Mostafa, A. A. F., Al-Askar, A. A. & Al-Otibi, F. O. Facile green synthesis of silver nanoparticles using aqueous leaf extract of Origanum majorana with potential bioactivity against multidrug resistant bacterial strains. *Crystals*. **12**, 603 (2022).
55. Rizwana, H., Alwhibi, M. S., Al-Judaie, R. A., Aldehaish, H. A. & Alsaggabi, N. S. Sunlight-mediated green synthesis of silver nanoparticles using the berries of Ribes rubrum (red currants): Characterisation and evaluation of their antifungal and antibacterial activities. *Molecules*. **27**, 2186 (2022).
56. Premasudha, P. et al. Biological synthesis and characterization of silver nanoparticles using Eclipta alba leaf extract and evaluation of its cytotoxic and antimicrobial potential. *Bull. Mater. Sci.* **38**, 965–973 (2015).
57. Rupiasih, N. N., Aher, A., Gosavi, S. & Vidyasagar, P. Green synthesis of silver nanoparticles using latex extract of Thevetia peruviana: a novel approach towards poisonous plant utilization. *Recent. Trends Phys. Mater. Sci. Technol.*, 1–10 (2015).
58. Shi, Z. et al. Cu immobilized on chitosan-modified iron oxide magnetic nanoparticles: Preparation, characterization and investigation of its anti-lung cancer effects. *Arab. J. Chem.* **14**, 103224 (2021).
59. Some, S. *et al.* Effect of feed supplementation with biosynthesized silver nanoparticles using leaf extract of Morus indica L. V1 on Bombyx mori L. (Lepidoptera: Bombycidae). *Sci. Rep.* **9**, 14839 (2019).
60. Saad, A. M. *et al.* Polyphenolic extracts from pomegranate and watermelon wastes as substrate to fabricate sustainable silver nanoparticles with larvicidal effect against *Spodoptera littoralis*. *Saudi J. Biol. Sci.* **28**, 5674–5683 (2021).
61. Selim, Y. A., Azb, M. A., Ragab, I. & El-Azim, H. M. A. Green synthesis of zinc oxide nanoparticles using aqueous extract of Deverra tortuosa and their cytotoxic activities. *Sci. Rep.* **10**, 3445 (2020).
62. Ying, S. et al. Green synthesis of nanoparticles: current developments and limitations. *Environ. Technol. Innov.* **26**, 102336 (2022).
63. Ahmed, S. F. et al. Green approaches in synthesising nanomaterials for environmental nanobioremediation: Technological advancements, applications, benefits and challenges. *Environ. Res.* **204**, 111967 (2022).
64. Ibrahim, M., Agboola, J., Abdulkareem, A., Adedipe, O. & Tijani, J. In *IOP Conference Series: Materials Science and Engineering.* 012022 (IOP Publishing).
65. Nyakundi, E. O. & Padmanabhan, M. N. Green chemistry focus on optimization of silver nanoparticles using response surface methodology (RSM) and mosquitocidal activity: Anopheles Stephensi (Diptera: Culicidae). *Spectrochim. Acta Part A Mol. Biomol. Spectrosc.* **149**, 978–984 (2015).
66. Chou, K. S., Lu, Y. C. & Lee, H. H. Effect of alkaline ion on the mechanism and kinetics of chemical reduction of silver. *Mater. Chem. Phys.* **94**, 429–433 (2005).

67. Zuorro, A., Iannone, A., Miglietta, S. & Lavecchia, R. Green synthesis of silver nanoparticles using spent coffee ground extracts: Process modelling and optimization. *Nanomaterials* **12**, 2597 (2022).
68. Manosalva, N. *et al.* Green synthesis of silver nanoparticles: Effect of synthesis reaction parameters on antimicrobial activity. *World J. Microbiol. Biotechnol.* **35**, 1–9 (2019).
69. Kareem, E. A. A., Sultan, A. E. & Oraibi, H. M. Synthesis and characterization of silver nanoparticles: A review. *Ibn AL-Haitham J. Pure Appl. Sci.* **36**, 177–200 (2023).
70. Song, J. Y. & Kim, B. S. Rapid biological synthesis of silver nanoparticles using plant leaf extracts. *Bioprocess Biosyst. Eng.* **32**, 79–84 (2009).
71. Abbas, Q. *et al.* Green synthesis of silver nanoparticles using Bidens frondosa extract and their tyrosinase activity. *Iran. J. Pharm. Res. IJPR* **16**, 763 (2017).
72. Pungle, R. et al. Green synthesis of silver nanoparticles using the Tridax Procumbens plant extract and screening of its antimicrobial and anticancer activities. *Oxid. Med. Cell. Longev.* (2022).
73. Chetia, L., Kalita, D. & Ahmed, G. A. Synthesis of Ag nanoparticles using diatom cells for ammonia sensing. *Sens. Bio-Sens. Res.* **16**, 55–61 (2017).
74. Makarov, V. *et al.* Green nanotechnologies: synthesis of metal nanoparticles using plants. *Acta Nat. (англоязычная версия)* **6**, 35–44 (2014).
75. Ahmed Naseer, M. I., Ali, S., Nazir, A., Abbas, M. & Ahmad, N. Green synthesis of silver nanoparticles using Allium cepa extract and their antimicrobial activity evaluation. *Chem. Int.* **8**, 89–94 (2022).
76. Panneerselvam, C. et al. Fern-synthesized nanoparticles in the fight against malaria: LC/MS analysis of Pteridium aquilinum leaf extract and biosynthesis of silver nanoparticles with high mosquitocidal and antiplasmodial activity. *Parasitol. Res.* **115**, 997–1013 (2016).
77. Alahmad, A. *et al.* Green synthesis of silver nanoparticles using *Hypericum perforatum* L. aqueous extract with the evaluation of its antibacterial activity against clinical and food pathogens. *Pharmaceutics* **14**, 1104 (2022).
78. Sun, Q. *et al.* Green synthesis of silver nanoparticles using tea leaf extract and evaluation of their stability and antibacterial activity. *Colloids Surf. A Physicochem. Eng. Aspects* **444**, 226–231 (2014).
79. Jongprakobkit, J., Wisaichon, W., Praditweangkum, W. A. & Simple and green approach for colorimetric ammonia determination by combining pervaporation with paper impregnated anthocyanins extracted from red cabbage. *Curr. Appl. Sci. Technol.* 394–407 (2020).

Acknowledgements

This study was supported by the Department of Occupational Health and Safety Engineering, School of Public Health and Safety, Shahid Beheshti University of Medical Sciences (Ethical code: IR.SBMU.PHNS.REC.1402.025).

Author contributions

M.A.R and R.Z: Study design, interpretation of the results, and drafting the manuscript, SH.F, H.E, and H.G: acquisition of data, S.F.D= Statistical analysis.

Declarations

Competing interests

The authors declare no competing interests.

Additional information

Supplementary Information The online version contains supplementary material available at https://doi.org/10.1038/s41598-024-73010-w.

Correspondence and requests for materials should be addressed to R.Z.